A Type III grouted seismic connector for precast concrete structures

Theresa C. Aragon, Yahya C. Kurama, and Donald F. Meinheit

- The Type III connector presented in this paper offers the potential for a high-performance yet simple nonproprietary, low-cost system that allows energy-dissipating bars under cyclic loading to reach close to their full ultimate (maximum) strength and strain capacity in tension over a short, grouted embedment length.
- The use of short grouted connections simplifies the construction of precast concrete structures because protruding bar lengths from precast concrete members are minimized and field-grouting lengths are reduced.
- Out of the six specimens tested, five bars achieved low-cycle fatigue fracture and one bar failed through ductile pullout at maximum strains close to the monotonic tension strain capacity corresponding to the ultimate (maximum) strength of the bar.

A hybrid precast concrete wall system with horizontal joints was recently validated[1–5] as a special shear wall according to the American Concrete Institute's (ACI's) *Building Code Requirements for Structural Concrete (ACI 318-14) and Commentary (ACI 318R-14)*[6] following the requirements given in ACI's *Acceptance Criteria for Special Unbonded Post-Tensioned Precast Structural Walls Based on Validation Testing and Commentary* (ACI ITG-5.1).[7] Similar systems with gap-opening joints have also been developed for precast concrete building frames and bridge piers.[8,9] An important component in these structures is the ASTM A706[10] energy-dissipating bars crossing the gap-opening joint between the foundation and base of the structure (for example, shear wall, column, and bridge pier bases). The energy-dissipating bars are designed[2,5] such that the tension strains at the maximum structural member drift are greater than $0.5\varepsilon_{uel}$ (to provide adequate energy dissipation) but do not exceed $0.85\varepsilon_{uel}$ (to prevent low-cycle fatigue fracture), where ε_{uel} is the uniform elongation strain of the energy-dissipating bar at ultimate (maximum) strength f_{uel} under monotonic tension loading. A predetermined length of each bar is unbonded from the concrete (by wrapping the bar with plastic) at the gap-opening joint to avoid concentrating nonlinear deformations over a short length of the bar and to ensure that the steel strains remain within the intended range.

Sufficient development length of the energy-dissipating bars is required for the bars to reach the expected tension strains without pullout under cyclic loading. In the hy-

brid precast concrete wall system that was validated, this objective could only be achieved by casting (at one end) and grouting (at the other end) the full ACI 318-14 development length of each energy-dissipating bar.[1–6] However, using the full development length required by ACI 318-14 results in long energy-dissipating bar lengths protruding out of the precast concrete base, creating challenges for production, transportation, and erection.

To address the issue of long development lengths for the energy-dissipating bars, Smith et al.[3,5] used a Type II grouted mechanical splice system in the foundation of one of the six wall specimens tested in their experimental program (specimen HW2). Type II splices are a commonly used detail in precast concrete construction and are allowed in seismic regions of the United States by section 5.4.2 of ACI ITG-5.2.[11] The use of short, grouted Type II splices can simplify the construction of precast concrete structures by allowing the energy-dissipating bars to be precast into the member with only a short bar length protruding out for field grouting into a splice sleeve cast into the top of the foundation. However, the Type II splices in specimen HW2 were unable to withstand the large gap-opening deformations at the base of the structure, causing the system to fail prematurely due to bond pullout of the energy-dissipating bars from the splice sleeve, preventing the ACI ITG-5.1 validation of the wall.

The Type II splices used in the wall specimen met all ACI 318-14 and AC133[12] requirements, and the grout for the splices met the splice manufacturer's specifications.[3,5] The reason for the splice failures was that energy-dissipating bars tested in precast concrete structures per ACI ITG-5.1 undergo much greater strains over a significantly larger number of cycles than the strain history required to classify a Type II mechanical connector system per AC133.[12] Therefore, Smith and Kurama[2] suggested that for the development length of the energy-dissipating bars "Sufficient development length or anchorage should be provided at both ends of the wrapped region of the energy-dissipating bars. Due to the large reversed-cyclic steel strains expected through Δ_{wm}, Type II grouted mechanical splices specified in section 21.1.6 of ACI 318-11 and permitted by section 5.4.2 of ACI ITG-5.2 should not be used for the energy-dissipating bars in hybrid precast concrete walls in seismic regions unless the splices have been tested and validated under cyclic loading up to a steel strain of at least $0.85\varepsilon_{su}$." (Δ_{wm} is maximum-level wall drift corresponding to maximum-considered earthquake, and ε_{su} in Smith and Kurama[2] is the same as ε_{uel} defined in this paper.) In response

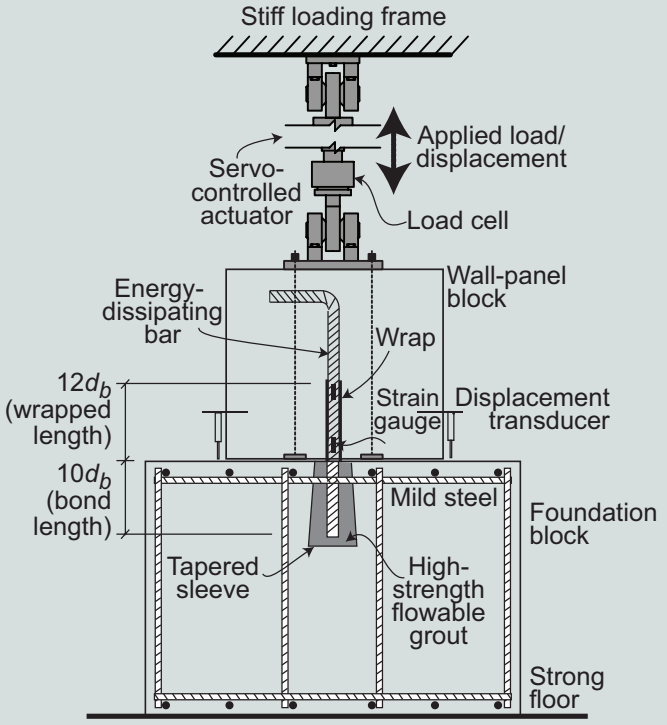

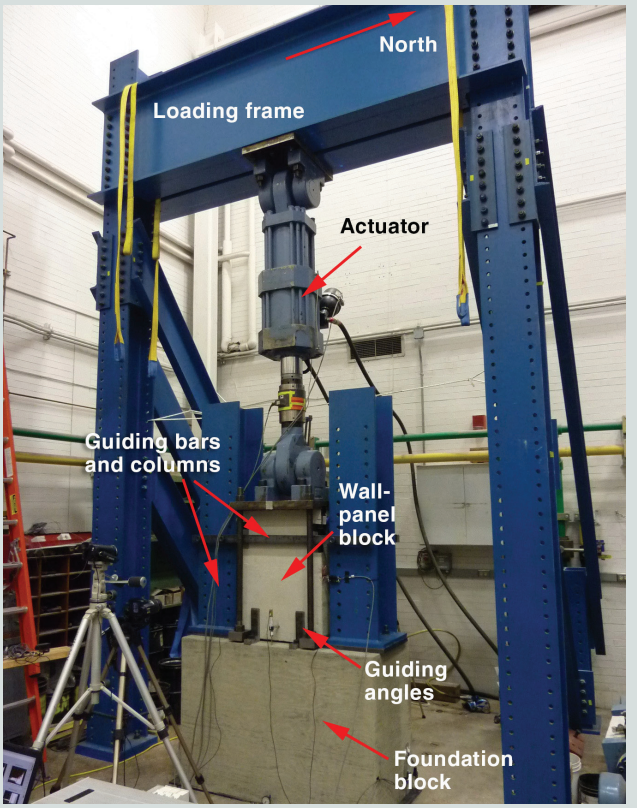

Figure 1. Energy-dissipating bar connection test setup. Note: Figure not to scale. d_b = bar diameter.

to the need for a higher-performing connection (referred to here as Type III) for anchoring energy-dissipating bars, this paper discusses the results from investigating the use of a new type of tapered cylindrical grouted seismic connector for six energy-dissipating bar specimens.

Test setup

Figure 1 shows the test setup used in the Type III connector experiments. The foundation and wall-panel blocks were cast separately and then connected using a single grouted connector at the center of the foundation and wall panel. The foundation block (**Fig. 2**), which had a width w_f of 24 in. (610 mm), height h_f of 36 in. (910 mm), and length l_f of 54 in. (1370 mm), was designed to represent the foundation in a precast concrete wall system. The height of the foundation block was designed to accommodate two energy-dissipating bar connector sleeves, one on top and one on the bottom of the block. This allowed the foundation block to be reused in two separate tests by turning the block over.

The wall-panel block (**Fig. 3**), which had a thickness t_w of 15 in. (380 mm), height h_w of 32 in. (810 mm), and length l_w of 24 in. (610 mm), was designed to represent a slice over the length of a precast concrete wall panel at the base. The deformed Grade 60 (414 MPa) ASTM A615[13] reinforcement placed within the block was similar to that found around the energy-dissipating bars in a hybrid precast concrete wall base panel.[2] A no. 7 (22M; nominal diameter d_b of 0.875 in. [22.2 mm]) Grade 60 ASTM A706 reinforcing bar served as the energy-dissipating bar to connect the wall panel and foundation blocks in all six tests. The energy-dissipating bar was cast at the center of the wall-panel block with a standard 90-degree hook to fully anchor the bar. (This hook would not be needed in a full-height wall panel in practice.) The bar was unbonded from the concrete over a length l_{sw} of $12d_b$ (where d_b is the bar diameter and l_{sw} is equal to 10.5 in. [270 mm] for a no. 7 bar) at the bottom of the wall-panel block by wrapping it with plastic. The unbonded (wrapped) portion of the energy-dissipating bar (frequently referred to as

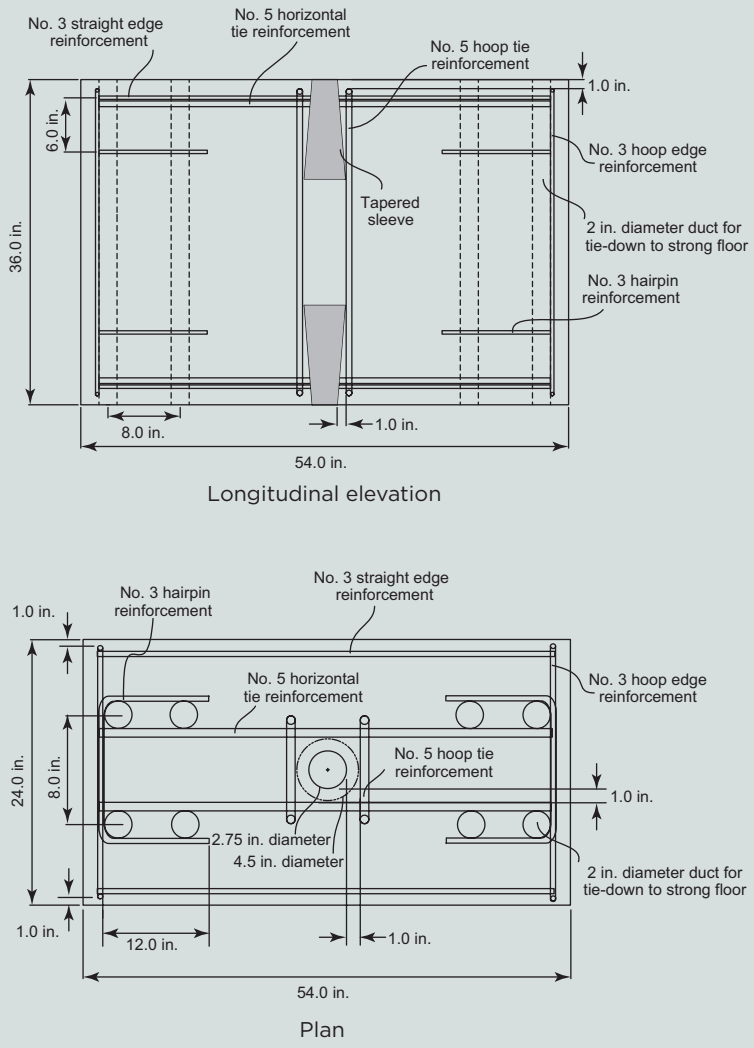

Figure 2. Foundation block. Note: no. 3 = 10M; no. 5 = 16M; 1 in. = 25.4 mm.

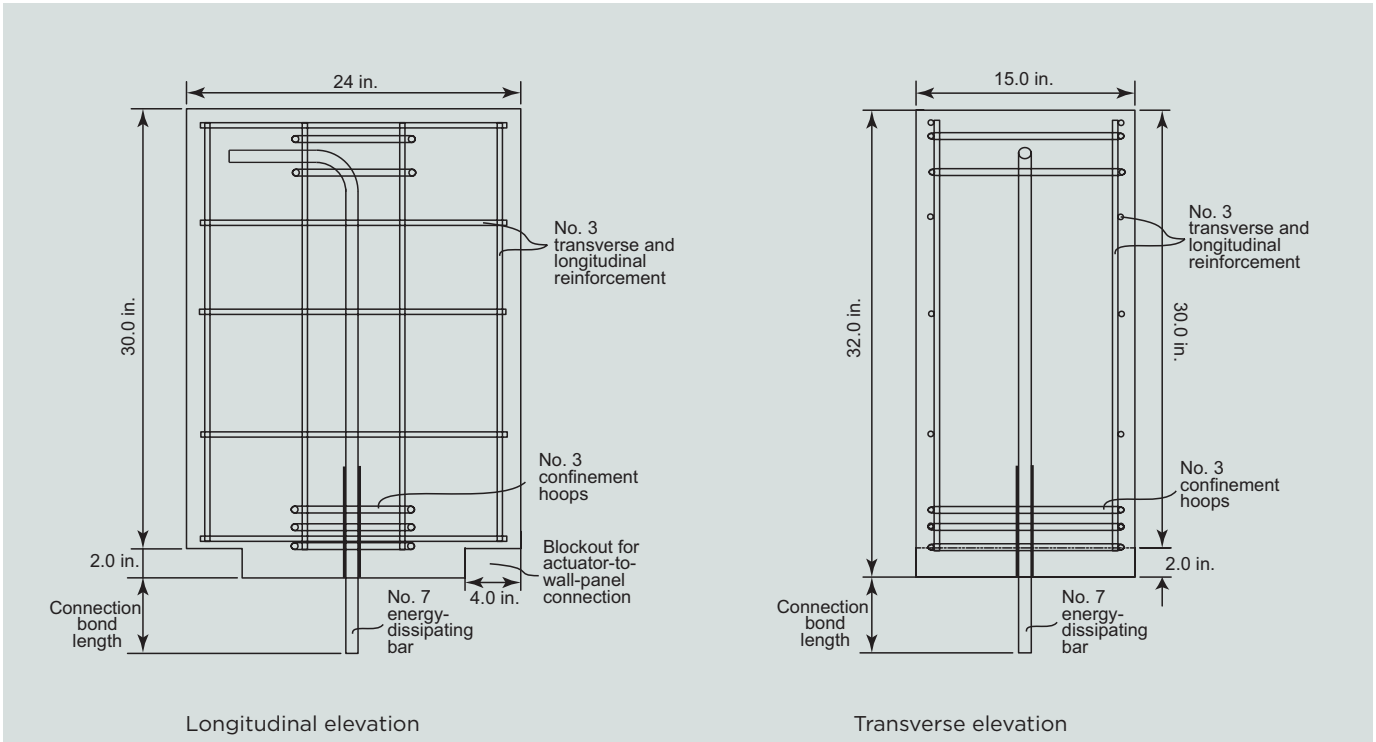

Figure 3. Wall-panel block. Note: no. 3 = 10M; no. 7 = 22M; 1 in. = 25.4 mm.

the stretch length), which is a typical feature to limit the maximum steel strains in hybrid precast concrete systems, was long enough to result in significant elongation of the bar before fracture (and therefore allow measurable separation at the joint between the wall-panel block and the foundation block). The unbonded portion of the energy-dissipating bar was also long enough to reduce the effect of any additional bar debonding (due to the cyclic loading of the bar) on the steel strains determined from the measured joint separation and the wrapped length (that is, any additional bar debonding length was small compared with the wrapped length).

During fabrication, the energy-dissipating bar protruded out of the bottom of the wall-panel block over the specified connection bond length. The cement-based, high-strength, flowable grout was mixed and placed manually up to a predetermined depth from the top of the connector sleeve at the top of the foundation block. Then the connection between the wall-panel and foundation blocks was achieved by embedding the protruding length of the energy-dissipating bar within the grout inside the connector sleeve.

The original grout depth inside the sleeve is a function of the energy-dissipating bar size and the connector sleeve geometry and was determined such that the grout cone would rise to the top of the connector sleeve upon full embedment of the energy-dissipating bar. To allow the energy-dissipating bar to be loaded into a small amount of compression strain without the wall-panel block making contact with the foundation block, a small initial gap was created using 0.015 in. (0.38 mm) thick temporary steel shims at the horizontal joint between the two blocks.

Design of tie reinforcement around energy-dissipating bar connector

Deformed ASTM A615 Grade 60 (414 MPa) vertical and horizontal tie reinforcement was placed around each connector sleeve inside the foundation to prevent breakout of the concrete surrounding the connection. A strut-and-tie model was used to proportion the vertical and horizontal reinforcing bars (**Fig. 4**). From vertical equilibrium, the total force in the vertical U-bar tie reinforcement ΣT_v (equal to $\Sigma A_v f_y$) within the effective connection zone is equal to the tension force in the energy-dissipating bar T_{ED} (equal to $A_{ED} f_{uel}$).

$$\sum T_v = T_{ED} \Rightarrow \sum A_v = \frac{A_{ED} f_{uel}}{f_y}$$

where

T_v = tension force in a vertical tie bar around the connector sleeve

A_v = area of a vertical tie bar around the connector sleeve

A_{ED} = area of the energy-dissipating bar

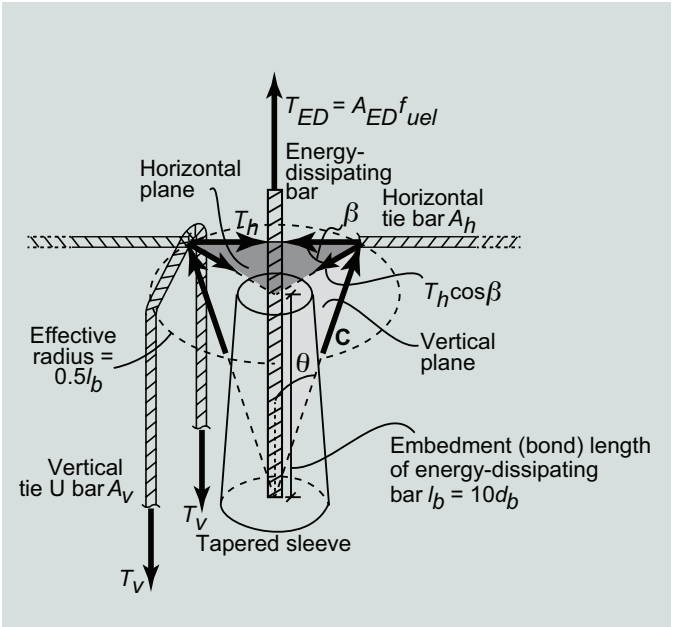

Figure 4. Strut-and-tie model for design of tie reinforcement around energy-dissipating bar connector. Note: A_{ED} = area of energy-dissipating bar; A_h = area of horizontal tie bar around connector sleeve; A_v = area of vertical tie bar around connector sleeve; f_{uel} = ultimate (maximum) strength of energy-dissipating bar under monotonic tension loading; l_b = energy-dissipating bar embedment (bond) length; T_{ED} = tension force in energy-dissipating bar; T_h = tension force in horizontal tie bar; T_v = tension force in vertical tie bar; β = angle of horizontal plane in strut-and-tie model; θ = angle of vertical plane in strut-and-tie model.

f_{uel} = measured ultimate (maximum) strength of the energy-dissipating bar under monotonic tension loading

f_y = specificed yield strength of the tie reinforcement

Similarly, the total required horizontal tie steel area within the effective connection zone ΣA_h can be calculated as

$$\sum A_h = \frac{A_{ED} f_{uel} \tan\theta}{2 f_y \cos\beta}$$

where

θ = angle of the vertical plane in the strut-and-tie model

β = angle of the horizontal plane in the strut-and-tie model

To test the limits of the design, no capacity reduction factor was used in determining the tie steel reinforcement for the specimens. Because of the testing of two connectors in each foundation block, closed hoops (Fig. 2) rather than U bars were used as the vertical tie reinforcement. Based on section R17.4.2.9 (Anchoring to Concrete) of ACI 318-14, only the tie bars placed within an effective connection radius (measured from the energy-dissipating bar centerline) of 0.5 times the energy-dissipating bar embedment (bond) length l_b of $10d_b$ were considered effective. Also, the angle of the vertical plane in the strut-and-tie model θ was approximated as $\tan^{-1}[(0.5l_b)/l_b] \approx 30$ degrees. The angle β of the horizontal plane (dark shaded region in Fig. 4) was assumed to be 45 degrees. This design approach was evaluated in the tests by measuring the strains in the tie reinforcement.

Energy-dissipating bar connection properties

Figure 5 shows the connector sleeves (ducts) used in the six tests and **Table 1** gives their properties. The sleeves were made by a local sheet metal fabricator using 25-gauge (0.0209 in. [0.53 mm] thick), smooth sheet metal. The sleeves were slightly longer than the connection bond length of the energy-dissipating bars for practical tolerance purposes. The sleeve diameter at the top of the foundation block was chosen to provide enough clearance and tolerance for the no. 7 (22M) energy-dissipating bar. The same high-strength cementitious grout product (meeting the requirements of ASTM C1107[14]) was used in all six tests. For each connection, a 55 lb (25 kg) bag of prepackaged grout was mixed per the manufacturer's instructions to reach a flowable consistency. The flow diameter (spread) of each batch was measured using a 2 in. (50 mm) diameter × 4 in. (100 mm) tall plastic tube that was filled with grout and slowly lifted on top of a flow template. The target grout spread was 5 to 6 in. (130 to 150 mm). The compression strength of the grout at 28 days and on the day of energy-dissipating bar connection testing was determined as the average from a minimum of three 2 × 2 in. grout cubes. Although a reasonably consistent grout spread diameter of 5 to 6 in. was achieved for the six connections, there were considerable differences in the grout strength even at a consistent age of 28 days (**Table 2**).

The connector sleeve in specimen 1 had a length of 11 in. (280 mm), a taper angle θ_d of 4.5 degrees (with a taper entrance inner diameter of 2.75 in. [69.9 mm] and bottom inner diameter of 4.5 in. [110 mm]), and a smooth (uncorrugated) surface. The bond length of the energy-dissipating bar was $10d_b$ (8.75 in. [222 mm] for a no. 7 [22M] bar).

Specimen 2 was used to investigate a longer bond length of $15d_b$ (13.125 in. [333 mm] for a no. 7 [22M] bar). Surface corrugations (deformations) were placed at approximately 1 in. (25 mm) spacing at the bottom and top of the connector sleeve to provide additional mechanical interlock for the grout cone. The taper angle θ_d was kept at 4.5 degrees (with a taper entrance inner diameter of 2.75 in. [69.9 mm] and bottom inner diameter of 5.25 in. [133 mm]). The sleeve length was increased to 15.75 in. (400 mm) to ac-

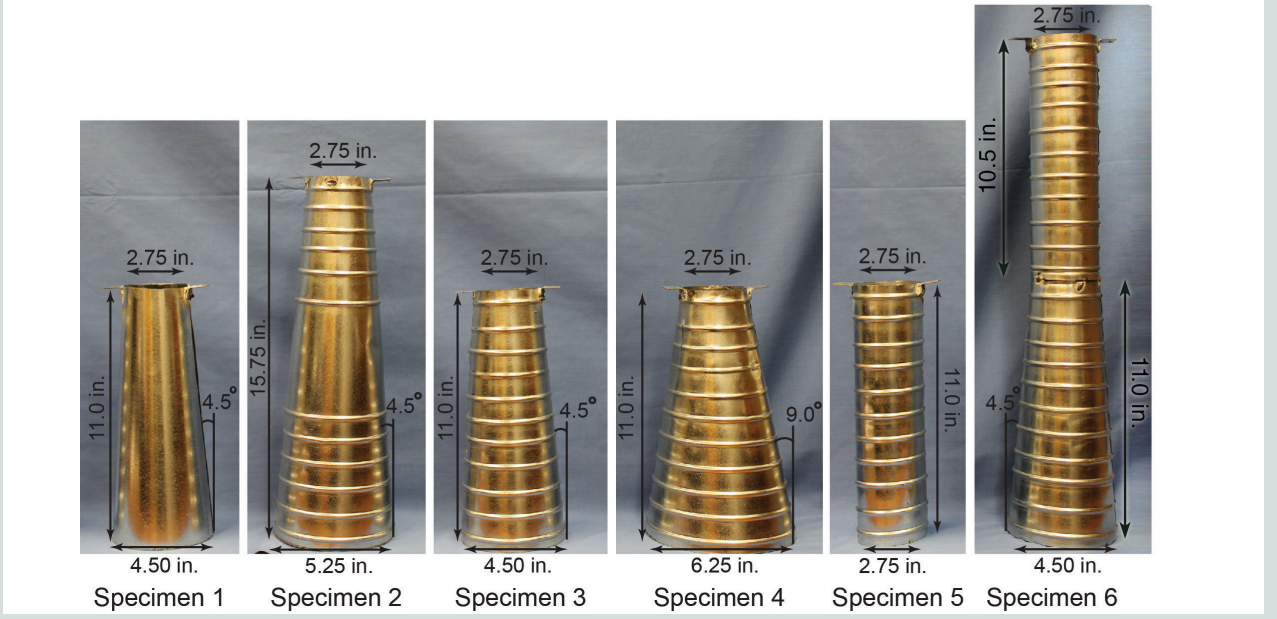

Figure 5. Connector sleeve dimensions. Note: 1 in. = 25.4 mm.

Table 1. Test parameters

Specimen	Connector sleeve					Energy-dissipating bar		
	Taper angle θ_d, degrees	Entrance diameter, in.	Bottom diameter, in.	Surface corrugations	Length, in.	Size	Wrapped length $l_{sw} = 12d_b$, in.	Bond length l_b, in.
1	4.5	2.75	4.5	None	11	No. 7	10.5	8.75
2	4.5	2.75	5.25	Spaced at 1 in.	15.75	No. 7	10.5	13.125
3	4.5	2.75	4.5	Spaced at 1 in.	11	No. 7	10.5	8.75
4	9.0	2.75	6.25	Spaced at 1 in.	11	No. 7	10.5	8.75
5	0.0	2.75	2.75	Spaced at 1 in.	11	No. 7	10.5	8.75
6	4.5 (option 2)	2.75	4.5	Spaced at 1 in.	11	No. 7	10.5	8.75

Note: l_b is equal to $15d_b$ for specimen 2 and $10d_b$ for all other specimens. Corrugations in specimen 2 were only placed within the top and bottom third of the sleeve length. d_b = bar diameter. No. 7 = 22M; 1 in. = 25.4 mm.

Table 2. Measured connector grout properties

Specimen	Grout product	Target 28-day compression strength, psi	Flow diameter, in.	Average 28-day compression strength $f'_{cg,28d}$, psi	Average test-day compression strength f'_{cg}, psi	Test-day age
1	GM1	8000	5	8912	9498	54
2	GM1	8000	5.5	8519	8631	124
3	GM1	8000	5.125	8931	8965	135
4	GM1	8000	5.25	9237	9515	41
5	GM1	8000	5.125	9908	10,324	48
6	GM1	8000	5.75	8642	9231	49

Note: 1 in. = 25.4 mm; 1 psi = 6.895 kPa.

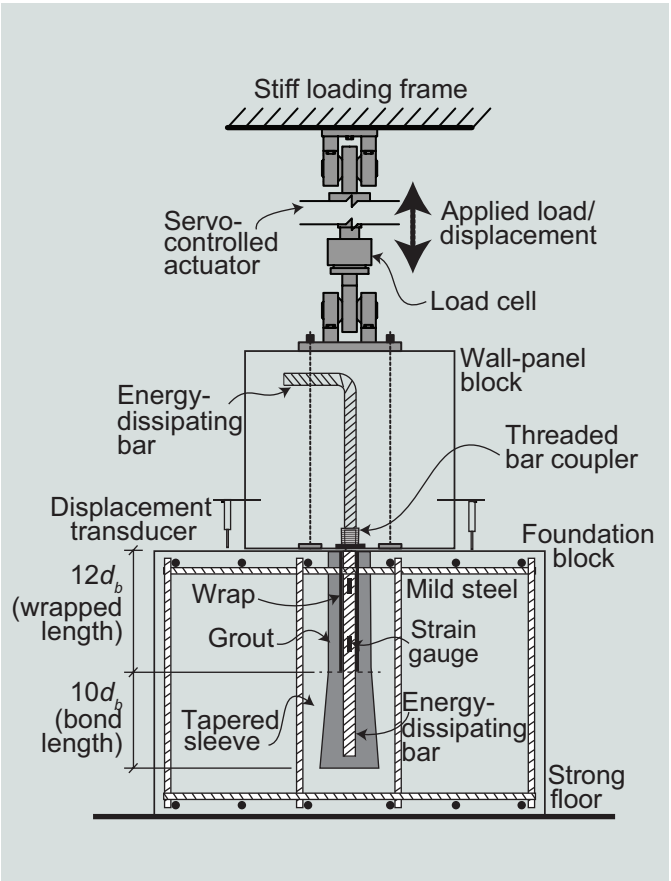

Figure 6. Option 2 connection test setup. Note: Figure not to scale. d_b = bar diameter.

commodate the longer energy-dissipating bar bond length. The average connection test-day grout strength f'_{cg} for this specimen (8631 psi [59.51 MPa]) was the lowest of the six specimens.

Specimen 3 had a sleeve with the same dimensions as specimen 1; however, this sleeve had surface corrugations at approximately 1 in. (25 mm) spacing throughout its length. The energy-dissipating bar bond length was kept at $10d_b$.

A larger sleeve taper angle θ_d of 9.0 degrees (with taper entrance inner diameter of 2.75 in. [69.9 mm] and bottom inner diameter of 6.25 in. [159 mm]) was investigated in specimen 4. Corrugations spaced at approximately 1 in. were also included on this sleeve.

A straight sleeve (θ_d equal to 0 degrees) with entrance and bottom inner diameter of 2.75 in. (69.9 mm) was investigated in specimen 5. The average connection test-day grout strength f'_{cg} for this specimen (10,324 psi [71.184 MPa]) was the highest of the six specimens.

To investigate the possibility of eliminating protruding bars out of the wall panel, the final specimen (specimen 6) included an ASTM A706 threaded dowel-bar coupler (splicer) cast into the bottom of the wall-panel block. **Figure 6** shows a drawing of this option 2 test specimen. To achieve the connection, the energy-dissipating bar was first threaded into the dowel-bar coupler according to manufacturer's specifications. Then the energy-dissipating bar was grouted into a sleeve cast inside the foundation below. The sleeve included a straight portion on top for the wrapped (unbonded) length of the energy-dissipating bar and a tapered portion for the connection bond length.

Loading

The foundation block was fixed to the laboratory strong floor, and the wall-panel block was connected to a servo-controlled hydraulic actuator supported by a stiff steel loading frame (Fig. 1). During testing, the hydraulic actuator was used to move the wall-panel block vertically to subject the energy-dissipating bar to a rigorous quasi-static cyclic axial strain history. The strain history varied slightly between tests but in general was consistent with the recommended loading for the validation of energy-dissipating bar connections in hybrid precast concrete walls.[2] **Figure 7** shows the strain history (solid line) that was the basis of loading in the tests. Also shown in the figure (dashed line) is the required strain history to certify Type II mechanical connector systems per AC133.[12] The strain history used in the testing of the Type III connectors herein was significantly more rigorous (both in amplitude and in number of cycles) than that required to certify a Type II connector.

The energy-dissipating bar was first subjected to 20 repeated cycles of loading, similar to the requirement in AC133[12] for Type II connectors. AC133 recommends loading to 95% of the specified yield strength of the bar during the

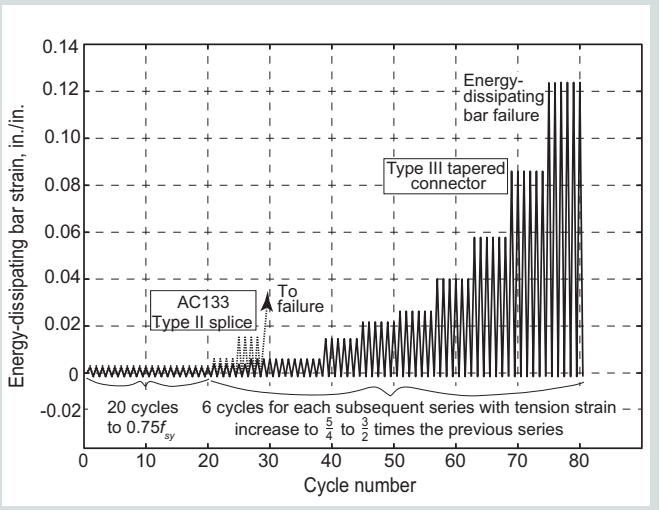

Figure 7. Target energy-dissipating bar strain history followed for testing of specimens. Note: f_{sy} = measured yield strength of energy-dissipating bar. 1 in. = 25.4 mm.

tension excursions of the first 20 cycles; however, for the tests conducted in this program, it was decided to load to 75% of f_{sy}, where f_{sy} is the measured yield strength of the energy-dissipating bar under monotonic tension, to ensure that the bar remained in the linear-elastic range. After reaching the peak tension stress in each cycle, the loading was reversed and a maximum compression stress of about 50% of f_{sy} was applied to the bar.

Following these initial 20 cycles, six cycles were applied in each subsequent loading series, with the tension strain amplitude increased to approximately $\frac{5}{4}$ to $\frac{3}{2}$ times the strain amplitude from the previous series. Upon reversal of the load, a small amount of compression strain was applied to the energy-dissipating bar until the two concrete blocks were in contact (simulating gap closing along the joint) and the compression strain in the bar no longer increased significantly. Testing continued until failure, with the objective of achieving ductile failure of the bar. Any specimen able to sustain six cycles at a peak tension strain of 0.06 in./in. (0.06 mm/mm) or greater was deemed to have undergone ductile failure, regardless of the eventual failure mode: either low-cycle fatigue fracture or bond pullout of the energy-dissipating bar. Because energy-dissipating bars satisfying ASTM A706[10] can show great variation in ε_{uel}, validation of connections based on a prescribed value of strain capacity rather than strain as a proportion of ε_{uel} results in more consistent requirements, regardless of the energy-dissipating bar used. Based on the test specimens in Smith et al.[1,3–5] and the full-scale design example in Smith and Kurama,[2] it was deemed that a reasonable target maximum energy-dissipating bar strain for the validation of the system as a Type III connector may be 0.06 in./in.

Instrumentation

Four linear variable displacement transducers were placed at midlength along the four edges of the horizontal joint to measure the relative vertical displacement between the wall-panel and foundation blocks. In addition, two strain gauges were placed on the wrapped length of the energy-dissipating bar and eight strain gauges were used on the tie reinforcement around the connector sleeve in the foundation block. To determine the stress in the energy-dissipating bar, the measured force in the hydraulic actuator was divided by the nominal bar area.

Because of the large elongation and strains reached in the energy-dissipating bar, the strain gauges on the bar failed relatively early during each test; therefore, the gap displacements from the four linear variable displacement transducers, measured throughout the test, were used to estimate the bar strains. An important factor for the energy-dissipating bar strains determined from the linear variable displacement transducers was the additional debonding that likely occurred at each end of the wrapped region of the bar under the cyclic loading history. As a result, the measured gap-opening displacement, when converted to strain on the wrapped length of the energy-dissipating bar, may overestimate the actual strain in the bar, potentially leading to an unconservative evaluation of the connection (that is, estimation of a greater strain capacity for the connection).

To address this discrepancy, the bar strains were estimated by dividing the average displacement (that is, relative joint displacement) from the four linear variable displacement transducers with an assumed total unbonded length l_{su} of $13d_b$ (that is, $12d_b$ of wrapped length plus an assumed $1d_b$ of additional debonding). Even though any additional debonding likely developed gradually throughout each test, this adjustment was applied to the entire strain history from the linear variable displacement transducers because the property of greatest interest was the largest tension strain (that is, connection strain capacity) toward the end of the test.

According to Smith and Kurama,[2] the total length of additional debonding expected to develop in an energy-dissipating bar during cyclic loading to $0.85\varepsilon_{uel}$ is approximately equal to $2d_b$ ($1d_b$ at each end of the wrapped region). However, this recommendation was based on the results of energy-dissipating bars across rocking joints in hybrid precast concrete walls.[4,5] The debonding length in bars subjected to pure axial loading (as in the testing of the energy-dissipating bar connections herein) may be smaller than the debonding length in bars subjected to combined axial and lateral loads (as in the rocking base joint of the hybrid walls tested by Smith et al.[4,5]). Further, visual evidence after the completion of the energy-dissipating bar connection tests indicated an additional debonding length of no more than $0.5d_b$ at the top of the foundation block. Because it was not possible to determine the amount of debonding at the other end of the wrapped length inside the wall-panel block, the same debonding length of $0.5d_b$ was assumed at both ends of the wrapped length, resulting in a total additional debonding length of $1d_b$.

Test results

Table 3 lists the results of the tests, including the total number of loading cycles sustained, accumulated strain, tension strain amplitude of last loading series (that is, last loading increment), number of cycles sustained in the last loading series, and failure mode. The accumulated strain represents the total amount of tension and compression strains (in absolute value) that each bar was subjected to during all of the sustained cycles. All of the presented strains are the adjusted strains (using l_{su} equal to $13d_b$) from the linear variable displacement transducer measurements described previously. Failure was deemed to have occurred during any loading cycle if there was a tension stress drop of 20% or greater from the largest tension stress reached

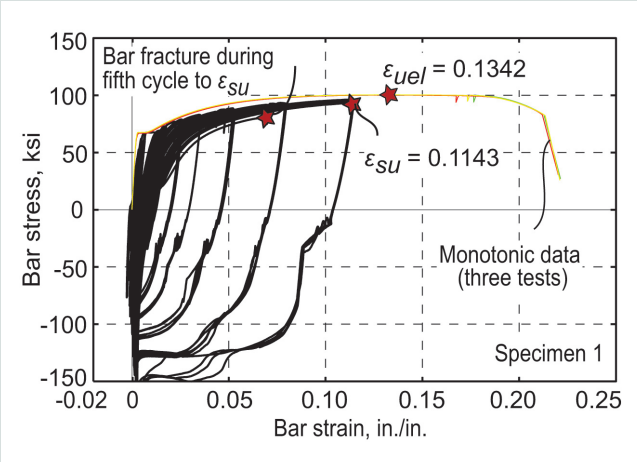

Specimen 1 (ductile fracture)

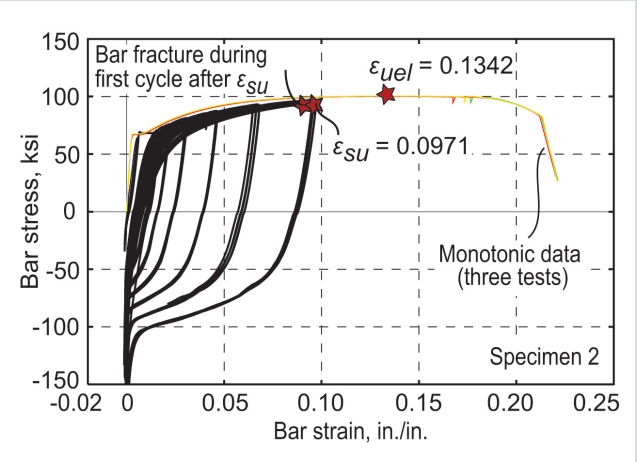

Specimen 2 (ductile fracture)

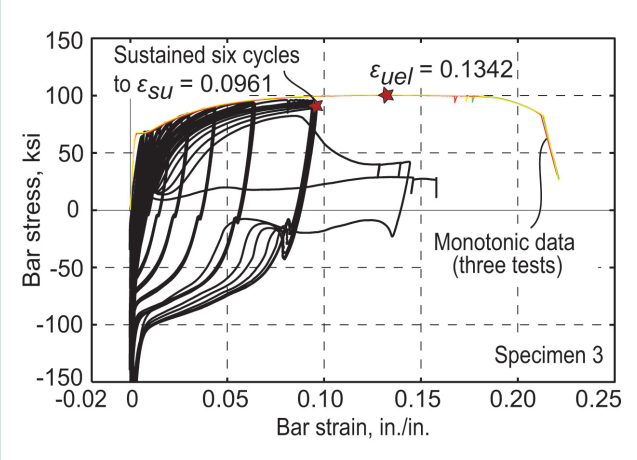

Specimen 3 (ductile pullout)

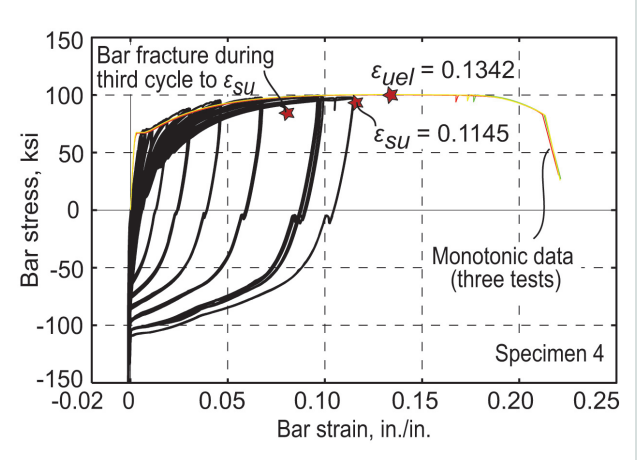

Specimen 4 (ductile fracture)

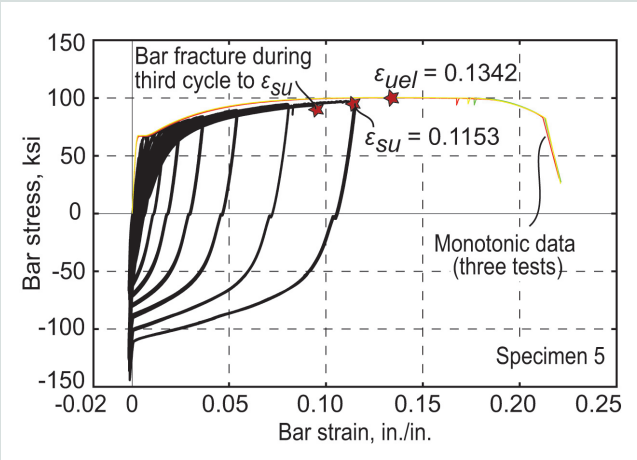

Specimen 5 (ductile fracture)

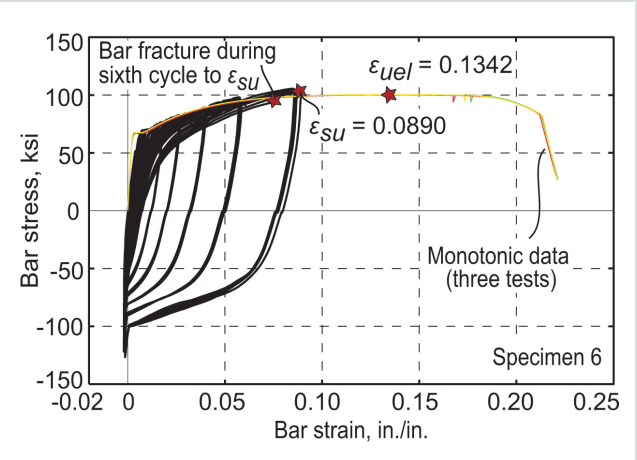

Specimen 6 (ductile fracture)

Figure 8. Energy-dissipating bar stress versus strain behavior under cyclic loading. Note: f_{uel} = measured ultimate (maximum) strength of energy-dissipating bar under monotonic tension loading; ε_{su} = maximum strain reached by energy-dissipating bar before connection failure; ε_{uel} = uniform elongation strain of energy-dissipating bar at f_{uel} under monotonic tension loading. 1 in. = 25.4 mm; 1 ksi = 6.895 MPa.

Table 3. Test results

Specimen	Total number of sustained cycles	Accumulated strain, in./in.	Strain amplitude of last series ε_{su}	Number of sustained cycles in last series	Failure mode
1	78	2.08	0.1143 ($0.85\varepsilon_{uel}$)	4	Ductile fracture
2	68	1.95	0.0971 ($0.72\varepsilon_{uel}$)	6	Ductile fracture
3	68	1.87	0.0961 ($0.72\varepsilon_{uel}$)	6	Ductile pullout
4	76	2.11	0.1145 ($0.85\varepsilon_{uel}$)	2	Ductile fracture
5	76	1.87	0.1153 ($0.86\varepsilon_{uel}$)	2	Ductile fracture
6	73	1.70	0.0890 ($0.66\varepsilon_{uel}$)	5	Ductile fracture

Note: f_{uel} = measured ultimate (maximum) strength of energy-dissipating bar under monotonic tension loading; ε_{su} = maximum strain reached by energy-dissipating bar before connection failure; ε_{uel} = uniform elongation strain of energy-dissipating bar at f_{uel} under monotonic tension loading. 1 in. = 25.4 mm.

in the entire loading history. Thus, the number of sustained cycles in Table 3 indicates the number of cycles during which at least 80% of the overall maximum tension stress was maintained. Any specimen able to sustain six cycles at a peak tension strain of 0.06 in./in. (0.06 mm/mm) or greater was deemed to have undergone ductile failure, due to either low-cycle fatigue fracture or bond pullout of the energy-dissipating bar.

The black lines in **Figure 8** show the measured cyclic stress versus strain behavior of the energy-dissipating bar specimens. Also shown in Fig. 8 are the measured monotonic tension stress versus strain behaviors of three bars from the same heat as the energy-dissipating bars used in the connections. All of the no. 7 (22M) energy-dissipating bars used in this phase of testing came from the same heat of steel. The bar strains in the monotonic tests were measured using an extensometer with a 2 in. (50 mm) gauge length. The resulting average uniform elongation strain ε_{uel} of the energy-dissipating steel at f_{uel} under monotonic tension loading was 0.1342 in./in. (0.1342 mm/mm).

The energy-dissipating bar in specimen 1 (Fig. 8) achieved ductile low-cycle fatigue fracture (without pullout) during the fifth cycle of the final series of cycles to a maximum strain ε_{su} of 0.1143 in./in. (0.1143 mm/mm) (approximately $0.85\varepsilon_{uel}$). During load reversal into compression, there were some irregularities in the energy-dissipating bar stress-strain behavior due to unintended rotations of the wall-panel block with respect to the foundation block. The guiding columns and bars in Fig. 1 were not present in the initial laboratory setup. The observed rotation was likely due to a small accidental eccentricity of the wall-panel block and the energy-dissipating bar with the actuator axis. As the wall-panel block rotated, it contacted the foundation block along one edge of the wall-panel block while the other edges were not in contact. This is most evident in the sudden increase in compression stiffness during the last series of cycles (Fig. 8). Subsequently, the wall-panel block rotated back to flat between the guiding angles, which were present in the initial laboratory setup, and the compression stiffness decreased because the wall-panel block was no longer in contact with the foundation block. There was another increase in stiffness toward the end of the compression loading, which was likely due to the wall-panel block contacting the small amount of grout that had bulged out (which is discussed later) from the connector sleeve during the loading of the bar in tension.

Due to the irregularities in how the load was transferred in compression, the measured stress-strain behavior in compression for specimen 1 (Fig. 8) does not reflect the true behavior of the energy-dissipating bar in compression. However, the behavior of the bar in tension was not affected. There was a slight bulging-out and deterioration of the grout at the top of the connector sleeve, but this did not affect the performance of the connection other than to increase the total unbonded length of the bar as discussed previously. **Figure 9** shows the bar fracture from specimen 1 as well as the slight grout bulging that was observed.

Following the testing of specimen 1, the laboratory setup was modified by placing guiding columns and bars to prevent any significant rotation of the wall-panel block. The smooth cyclic stress-strain behavior for specimen 2 (Fig. 8) verifies that the rotation of the wall-panel block was essentially eliminated. The energy-dissipating bar achieved ductile fracture (without pullout) during the first cycle after a complete series of six cycles to a maximum adjusted strain ε_{su} of 0.0971 in./in. (0.0971 mm/mm) (approximately $0.72\varepsilon_{uel}$).

The fracture strain capacity of $0.72\varepsilon_{uel}$ of this bar (and some of the other specimens tested subsequently, as described later) indicates that the maximum allowable strain of $0.85\varepsilon_{uel}$ recommended for the design of energy-dissipating bars in ACI ITG-5.2[11] may be too high and unconservative.

Like specimen 1, there was little deterioration in or around the tapered connector, with only a slight bulging-out of the grout at the top of the connector sleeve. No other damage was visible.

Figure 8 shows the measured cyclic stress-strain behavior for specimen 3, which was similar to specimen 1 except for the slightly lower compression strength of the connection grout (Table 2) and the presence of corrugations on the surface of the sleeve. The energy-dissipating bar in specimen 3 experienced progressive pullout during the loading cycles to a strain ε_{su} of 0.0961 in./in. (0.0961 mm/mm) (approximately $0.72\varepsilon_{uel}$), with the development of complete pullout (bond failure) after the completion of six cycles at this strain level (Fig. 9). This bond failure occurred in a ductile manner after significant nonlinear straining of the bar (Fig. 8). Because the bond failure occurred between the energy-dissipating bar and the surrounding grout, the corrugations on the connector sleeve surface were not effective and likely not necessary. These results demonstrate the importance of the grout in governing the failure mode of the connector and the resulting strain capacity.

Specimen 4 investigated a larger connector sleeve taper angle θ_d of 9.0 degrees. The energy-dissipating bar achieved ductile fracture (without pullout) during the third cycle of the final series of cycles to a maximum strain ε_{su} of 0.1145 in./in. (0.1145 mm/mm) (approximately $0.85\varepsilon_{uel}$) (Fig. 8). No bulging of the grout cone from the top of the connector sleeve was visible during or after the test, which may indicate that the increased taper angle was more effective in confining the grout cone inside the connector. However, because the larger taper angle would require larger connector spacing between multiple energy-dissipating bars, the taper angle θ_d of 4.5 degrees is believed to be more practical while still providing the desired connection performance.

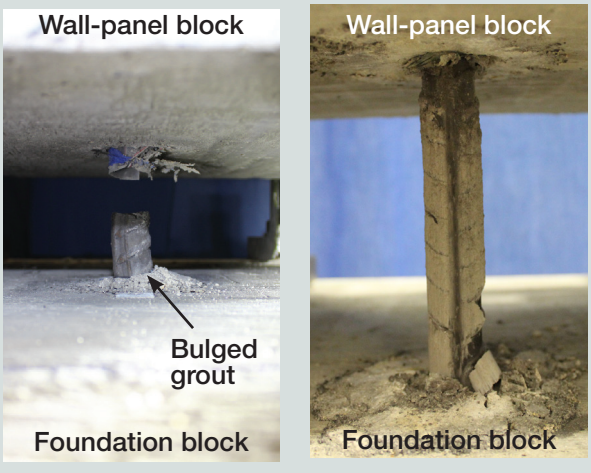

Low-cycle fatigue fracture (specimen 1)

Bond pullout (specimen 3)

Figure 9. Ductile connection failure examples.

To further explore the taper angle parameter, specimen 5 employed a straight sleeve with no taper (θ_d equal to 0 degrees). All other connection properties were kept the same, including the bond length for the energy-dissipating bar. The bar achieved ductile fracture (without pullout) during the third cycle of the final series of cycles to a maximum strain ε_{su} of 0.1153 in./in. (0.1153 mm/mm) (approximately $0.86\varepsilon_{uel}$) (Fig. 8). The compression strength of the grout (f'_{cg} equal to 10,324 psi [71.2 MPa]) in this specimen was the highest of all of the specimens tested (Table 2). The high performance (that is, bar fracture rather than pullout) achieved by the straight sleeve connector in specimen 5 may be the result of the high grout strength. This result again demonstrates the importance of the grout in governing the failure mode of the energy-dissipating bar and the connection strain capacity. While this connection failed in a desirable mode (ductile fracture without pullout), it may not be practical to require a grout compression strength of over 10,000 psi (69 MPa).

Specimen 6 was used to study an alternative connection scheme to eliminate protruding energy-dissipating bars from the wall panel by using a threaded bar coupler (splicer) together with a grouted tapered connector (option 2) (Fig. 6). The energy-dissipating bar achieved ductile fracture during the sixth cycle of the final series of cycles to a maximum strain ε_{su} of 0.0890 in./in. (0.0890 mm/mm) (approximately $0.66\varepsilon_{uel}$) (Fig. 8). The fracture of the bar occurred approximately 2 in. (50 mm) away from the threaded coupler, indicating that the coupler did not affect the performance of the specimen. The energy-dissipating bar had a tapered threaded end to match the coupler, resulting in the throat thickness of the threaded portion being smaller than the full bar diameter. Therefore, to strengthen the threaded portion, the end of the energy-dissipating bar was cold worked by the threaded coupler manufacturer. Although this configuration would be desirable in eliminating protruding energy-dissipating bars from the precast concrete member, it is important that the threaded couplers be aligned (that is, straight) and secured to the formwork to prevent misalignment during casting of the precast concrete member, which could cause the connector to become unusable.

None of the six specimens had any visible concrete cracking extending outward from the edge of the connector sleeve. The foundation block concrete compression strength $f'_{c,28d}$ was 6680 psi (46.1 MPa) at 28 days, which was greater than the specified strength of 4000 to 5000 psi (28 to 34 MPa). The tension strains in the vertical and horizontal tie reinforcement were small, also implying that the concrete did not crack. The largest tension strain measured

by the strain gauges on the vertical tie reinforcement was 6.414×10^{-4} in./in. (6.414×10^{-4} mm/mm) and the largest tension strain measured on the horizontal tie reinforcement was 1.403×10^{-4} in./in. (1.403×10^{-4} mm/mm), which are both considerably smaller than the yield strain of the bars. Similarly, no damage was visible on the wall-panel concrete for any of the six test specimens.

Conclusion

This paper presents the results from a series of six tests on the quasi-static cyclic axial load behavior of a novel Type III tapered, cylindrical cementitious-grouted connector for energy-dissipating deformed steel reinforcing bars at gap-opening joints in seismic precast concrete structures. All six specimens failed in a ductile manner after sustaining rigorous inelastic cyclic loading to maximum bar strains ranging from 0.0890 in./in. to 0.1153 in./in. (0.0890 mm/mm to 0.1153 mm/mm). These strains were developed in the energy-dissipating bar, which was anchored over a short, grouted bond length.

The test results demonstrate that a short, relatively simple cementitious-grouted connector has the capacity to develop energy-dissipating bars up to the large cyclic strain demands expected at gap-opening joints in high seismic regions. One specimen with slightly lower connector grout strength experienced ductile pull-out failure at the bar-to-grout interface. The other five specimens achieved ductile low-cycle fatigue fracture of the energy-dissipating bar.

The following conclusions can be made based on the results from these six tests using no. 7 (22M) energy-dissipating bars. Note that these conclusions may be limited to the specimens and materials tested (for example, energy-dissipating bar diameter and grout properties) as well as the applied loading conditions (uniaxial loading). Future tests using a wider range of parameters (for example, other bar sizes and grout products) as well as more realistic multidirectional loading conditions (that is, combined axial and lateral loads at a rocking joint with rotation) are needed before the results can be generalized. Other parameters that need to be tested include additional variations of the connector sleeve taper angle; connector edge distance; and construction tolerances, inaccuracies, and errors. The following specific conclusions can be drawn from the tests presented herein:

- The tested bond length of 10 times the bar diameter d_b was adequate to reach large cyclic energy-dissipating bar strains.
- Although the tested connector taper angle of 9.0 degrees resulted in less grout bulging from the sleeve, the smaller 4.5-degree taper angle is deemed more practical while still providing the desired connection performance.
- It is possible to eliminate the protruding length of an energy-dissipating bar from a precast concrete member by using a threaded bar coupler with a grouted tapered connector (specimen 6).
- Two of the specimens (specimens 2 and 6) experienced low-cycle fatigue fracture before reaching $0.85\varepsilon_{uel}$, which indicates that the maximum allowable strain of $0.85\varepsilon_{uel}$ recommended for the design of energy-dissipating bars in ACI ITG-5.2[11] may be unconservative.

Acknowledgments

This paper is based on work supported by a Daniel P. Jenny Fellowship and by a National Science Foundation Graduate Research Fellowship under grant no. DGE-1144468. The authors acknowledge the support of the PCI Research and Development Council, the PCI Central Region, and the members of the Project Advisory Panel, who include Ned Cleland of Blue Ridge Design, Tom D'Arcy of the Consulting Engineers Group, David Dieter of Mid-State Precast LP, Sameh El Ashri of e.construct Dubai, S.K. Ghosh of S.K. Ghosh Associates Inc., Harry Gleich of Metromont Corp., Neil Hawkins of the University of Illinois at Urbana-Champaign, Walter Korkosz of the Consulting Engineers Group, and Larbi Sennour of the Consulting Engineers Group. In addition, the following companies provided material donations and assistance to the project, and this support is gratefully acknowledged: StresCore Inc., Dayton Superior Corporation, and Erico Inc. The opinions, findings, conclusions, and recommendations expressed in the paper are those of the authors and do not necessarily represent the views of the individuals and organizations acknowledged.

References

1. Smith, B. J., Y. C. Kurama, and M. J. McGinnis. 2015. "Perforated Hybrid Precast Shear Walls for Seismic Regions." *ACI Structural Journal* 112 (3): 359–370.
2. Smith, B. J., and Y. C. Kurama. 2014. "Seismic Design Guidelines for Solid and Perforated Hybrid Precast Concrete Shear Walls." *PCI Journal* 59 (3): 43–49.
3. Smith, B. J., Y. C. Kurama, and M. J. McGinnis. 2013. "Behavior of Precast Concrete Shear Walls for Seismic Regions: Comparison of Hybrid and Emulative Specimens." *Journal of Structural Engineering* 139 (11): 1917–1927.
4. Smith, B. J., Y. C. Kurama, and M. J. McGinnis. 2011. "Design and Measured Behavior of a Hybrid Precast

Concrete Wall Specimen for Seismic Regions." *Journal of Structural Engineering* 137 (10): 1052–1062.

5. Smith, B. J., Y. C. Kurama, and M. J. McGinnis. 2012. "Hybrid Precast Wall Systems for Seismic Regions." Structural engineering research report NDSE-2012-01, Department of Civil and Environmental Engineering and Earth Sciences, University of Notre Dame, Notre Dame, IN. https://www3.nd.edu/~ykurama/REPORT_NDSE-12-01.pdf.

6. ACI (American Concrete Institute) Committee 318. 2014. *Building Code Requirements for Structural Concrete (ACI 318-14) and Commentary (ACI 318R-14)*. Farmington Hills, MI: ACI.

7. ACI Innovation Task Group 5. 2007. *Acceptance Criteria for Special Unbonded Post-Tensioned Precast Structural Walls Based on Validation Testing and Commentary*. ACI ITG-5.1. Farmington Hills, MI: ACI.

8. Joint ACI-ASCE (American Society of Civil Engineers) Committee 550. 2013. *Design Specification for Unbonded Post-Tensioned Precast Concrete Special Moment Frames Satisfying ACI 374.1*. ACI 550.3-13. Farmington Hills, MI: ACI.

9. Palermo, A., and S. Pampanin. 2008. "Enhanced Seismic Performance of Hybrid Bridge Systems: Comparison with Traditional Monolithic Solutions." *Journal of Earthquake Engineering* 12 (8): 1267–1295.

10. ASTM Subcommittee A01.05. 2016. *Standard Specification for Deformed and Plain Low-Alloy Steel Bars for Concrete Reinforcement*. ASTM A706/A706M. West Conshohocken, PA: ASTM International.

11. ACI Innovation Task Group 5. 2009. *Requirements for Design of a Special Unbonded Post-Tensioned Precast Shear Wall Satisfying ACI ITG-5.1 and Commentary*. ACI ITG-5.2. Farmington Hills, MI: ACI.

12. ICC-ES (ICC Evaluation Service). 2015. *Acceptance Criteria for Mechanical Connector Systems for Steel Reinforcing Bars*. AC133. Whittier, CA: ICC-ES.

13. ASTM Subcommittee A01.05. 2016. *Standard Specification for Deformed and Plain Carbon-Steel Bars for Concrete Reinforcement*. ASTM A615/A615M. West Conshohocken, PA: ASTM International.

14. ASTM Subcommittee C09.43. 2014. *Standard Specification for Packaged Dry, Hydraulic-Cement Grout (Nonshrink)*. ASTM C1107/C1107M. West Conshohocken, PA: ASTM International.

Notation

A_{ED} = area of energy-dissipating bar

A_h = area of horizontal tie bar around connector sleeve

A_v = area of vertical tie bar around connector sleeve

d_b = diameter of energy-dissipating bar

$f'_{c,28d}$ = average compression strength of foundation and wall-panel block concrete at 28 days

f'_{cg} = average compression strength of connector grout at day of energy-dissipating bar testing

$f'_{cg,28d}$ = average compression strength of connector grout at 28 days

f_{sy} = measured yield strength of energy-dissipating bar under monotonic tension loading

f_{uel} = measured ultimate (maximum) strength of energy-dissipating bar under monotonic tension loading

f_y = specified yield strength of tie reinforcement

h_f = height of foundation block

h_w = height of wall-panel block

l_b = embedment (bond) length of energy-dissipating bar

l_f = length of foundation block

l_{su} = total unbonded length of energy-dissipating bar (that is, wrapped length plus additional debonded length expected under cyclic loading)

l_{sw} = wrapped length of energy-dissipating bar

l_w = length of wall-panel block

t_w = thickness of wall-panel block

T_{ED} = tension force in energy-dissipating bar

T_h = tension force in horizontal tie bar

T_v = tension force in vertical tie bar

w_f = width of foundation block

β = angle of horizontal plane in strut-and-tie model

Δ_{wm} = maximum-level wall drift corresponding to maximum-considered earthquake

ε_{su} = maximum strain reached by energy-dissipating bar before connection failure

ε_{uel} = uniform elongation strain of energy-dissipating bar at f_{uel} under monotonic tension loading

θ = angle of vertical plane in strut-and-tie model

θ_d = taper angle of energy-dissipating bar connector sleeve

ΣA_h = total required area of horizontal tie reinforcement around connector sleeve

ΣA_v = total required area of vertical tie reinforcement around connector sleeve

About the authors

Theresa Aragon, MS, is a PhD candidate in the Department of Civil and Environmental Engineering and Earth Sciences at the University of Notre Dame in Notre Dame, Ind.

Yahya Kurama, PhD, PE, is a professor in the Department of Civil and Environmental Engineering and Earth Sciences at the University of Notre Dame.

Donald Meinheit, PhD, PE, SE, is a principal at Wiss, Janney, Elstner Associates Inc. in Chicago, Ill.

Abstract

The results from an experimental investigation of a novel tapered, cylindrical grouted Type III connector for ductile, energy-dissipating, deformed reinforcing bars in gap-opening joints of seismic precast concrete structures are presented. This Type III connector offers the potential for a high-performance yet simple, nonproprietary, low-cost system that allows energy-dissipating bars under cyclic loading to reach close to their full ultimate strength and strain capacity in tension over a short, grouted embedment length. The use of short grouted connections simplifies the construction of precast concrete structures because protruding bar lengths from precast concrete members are minimized and field-grouting lengths are reduced. Six energy-dissipating bar specimens were subjected to a rigorous uniaxial cyclic loading history inside a grouted sleeve. Five of the bars achieved ductile fracture (without pullout) and one bar (with slightly lower connector grout strength) failed through ductile pullout at maximum strains close to the monotonic tension strain capacity corresponding to the ultimate (maximum) strength of the bar.

Keywords

Connection, deformed reinforcing bar, energy-dissipating steel bar, gap-opening joint, grouted seismic connector, low-cycle fatigue fracture, pull-out (bond) failure, reinforcing bar, Type III connection, uniform elongation strain.

Review policy

This paper was reviewed in accordance with the Precast/Prestressed Concrete Institute's peer-review process.

Reader comments

Please address reader comments to journal@pci.org or Precast/Prestressed Concrete Institute, c/o *PCI Journal*, 200 W. Adams St., Suite 2100, Chicago, IL 60606.